Relative Conductances of Alkaneselenolate and Alkanethiolate Monolayers on Au{111}

Jason D. Monnell,[†,‡] Joshua J. Stapleton,[§] Shawn M. Dirk,[⊥] William A. Reinerth,[⊥] James M. Tour,[*,⊥] David L. Allara,[*,§] and Paul S. Weiss[*,†]

Departments of Chemistry and Physics and Departments of Chemistry and Materials Science and Engineering, 104 Davey Laboratory, The Pennsylvania State University, University Park, Pennsylvania 16802-6300, and Department of Chemistry and Center for Nanoscale Science and Technology, Rice University, Houston, Texas 77005

Received: December 21, 2004; In Final Form: August 16, 2005

The electronic properties of alkanethiolate [$CH_3(CH_2)_nS-$, $n = 9$ and 11] and alkaneselenolate [$CH_3(CH_2)_n$-$Se-$, $n = 9$ and 11] self-assembled monolayers on Au{111} have been quantitatively compared. Simultaneously acquired apparent tunneling barrier height (ATBH) and scanning tunneling microscopy (STM) images reveal that alkanethiolate molecules have a lower barrier to tunneling, and therefore a higher conductance than alkaneselenolates of the same alkyl chain length. Molecular and contact conductance differences were elucidated by using observed STM topographic tunneling height differences between the analogous species. This apparent topographic difference combined with comparative ATBH data indicate that the observed decrease in conductance for alkaneselenolates compared to alkanethiolates originates exclusively from the Au-chalcogenide physical, chemical, and electronic contact.

Introduction

Molecule−substrate contact conductance is an important property to consider in designing molecular electronic devices.[1,2] There are several headgroup choices available to bind potential molecular devices to metal surfaces, including chalcogens (O, S, Se, and Te),[3−5] isonitrile,[6,7] and direct C−metal bonds.[8] The most studied are the chalcogens, particularly sulfur, since it forms a strong bond with many metal surfaces. Calculations predicting the conductance differences between the chalcogens on Au differ as to whether S or Se has the larger contact conductance.[9,10] Conductance measurements at the single molecule scale remain difficult to perform. Conductance measurements of self-assembled monolayers (SAMs) of a variety of molecules with different headgroups have been performed by using conductive probe atomic force microscopy with and without nanoparticle contacts to the probe tip,[11−13] nanorod in-wire junctions,[14−17] and magnetically controlled crossed wire junctions.[18] All these experiments, however, typically address many molecules, electrically connecting to them by using a metal nanoparticle or physical touch, each of which could add complexity to understanding the measurement. Recently, Xu and Tao reported break junction measurements of single molecule resistances of selected bifunctional molecules by repeatable formation and breakage of junctions between a molecule and two gold electrodes.[19] While providing calibrated molecular resistances, this technique is experimentally labor intensive, and only a limited variety of molecules can be probed, one molecule at a time. In addition, the conductance of single molecules bridged between fabricated rigid junctions has been measured,[20,21] but these measurements are difficult, requiring arduous fabrication processing with relatively low yields, and are not suitable to direct, quantitative comparisons between different molecules. On the other hand, using scanning tunneling microscopy (STM) to probe mixed SAMs allows side by side relative conductance measurements of single molecules. At the same time, local surface effects arising from local packing and surface features can be taken into account, thus yielding a better understanding of molecular conductance.

To understand the properties of molecule−metal contacts, contributions to the molecule's conductance from each of its components, e.g., the "backbone" and headgroup at each contact, need to be determined independently. To achieve this, a series of experiments designed to measure the tunneling current decay through molecules adsorbed to a surface were performed with a combination of constant current topographic STM and apparent tunneling barrier height (ATBH) imaging. In this paper, S is shown to be a more conductive headgroup than Se in alkanechalcogenide SAMs on Au{111} by data from simultaneous topographic STM and ATBH imaging, in conjunction with interpretation via a two-barrier tunneling model.[22,23]

Experimental Section

Mixed SAMs of alkanethiolates and alkaneselenolates were prepared on Au{111} deposited on mica (Molecular Imaging Inc., Tempe, AZ). Decyl and dodecyl backbones for both headgroup moieties were used. Alkanethiolate SAMs were deposited from 1 mM ethanolic solutions of the alkanethiol, while alkaneselenolates were deposited from 0.2 mM ethanolic solutions of dialkyl-diselenide. Mixed monolayers were deposited by mixing solutions stoichiometrically, taking into account that two selenolate molecules are deposited for each dialkyl-diselenide. The resultant surface coverage reflected the deposition solution composition as shown by STM images in which two types of image features were consistently observed and

* To whom correspondence should be addressed. P.S.W.: stm@psu.edu.
[†] Departments of Chemistry and Physics, The Pennsylvania State University.
[‡] Current address: Civil and Environmental Engineering Department, 949 Benedum Hall, The University of Pittsburgh, Pittsburgh, PA 15260.
[§] Departments of Chemistry and Materials Science and Engineering, The Pennsylvania State University.
[⊥] Department of Chemistry and Center for Nanoscale Science and Technology, Rice University.

10.1021/jp044186q CCC: $30.25
Published on Web 10/11/2005

could be correlated with solution composition. All samples were deposited for 24 h at 70 °C. Alkanethiols were obtained from Sigma-Aldrich (used as received), while dialkyl-diselenide molecules were prepared according to previously reported methods.[24,25] All constant current STM experiments were carried out as previously described under ambient conditions at sample biases of ±1 V and tunneling currents between 0.5 and 3.0 pA, using custom-built instrumentation.[26] Topographic height calibration was performed prior to and after experiments with Au steps and vacancy islands as internal standards yielding an error of ±0.1 Å. ATBH data were acquired by using a 30 mV rms 3.75 kHz AC voltage attenuated by 20 dB to modulate the tip−sample separation by ~0.3 Å, resulting in a modulated tunneling current. The modulated tunneling current is detected by using a lock-in amplifier, which yields a measure of d*I*/dz, thus the ATBH.[27−30] Since the voltage modulation frequency is well above the feedback loop bandwidth (~2 kHz), there is a negligible effect on the measured constant current topography map. Average values for ATBH were obtained by identifying individual molecules of each species in each image, and taking the average value for the maxima of each identifiable molecule.

Results and Discussion

Apparent Topographic Height Differences and the Two-Barrier Tunneling Model. An analytical description of tunneling through a molecule and its relationship to apparent topography is needed to design an experiment to assess the difference between molecular contacts on conductance. For a molecule attached to a surface being locally probed via STM, a tunneling electron transits three regimes: the gap between the tip and sample, the backbone of the molecule, and the headgroup junction to the substrate, as illustrated in Figure 1. Each of these parts contributes to the conductance of the system. The overall conductance (G_t) of a molecule can be described as a product of exponential decays of current through the tip−sample gap (G_{gap}, eq 1) and along the methylene backbone ($G_{backbone}$, eq 2), and factors for contact conductances A (between the tip and molecule) and B (between the molecule and substrate) as in eq 3.[22,23,31]

$$G_{gap} = Ae^{-\alpha d_{gap}} \quad (1)$$

$$G_{backbone} = Be^{-\beta L_{backbone}} \quad (2)$$

$$G_t = G_{gap}G_{backbone} = ABe^{-\beta L_{backbone}}e^{-\alpha d_{gap}} \quad (3)$$

The exponential tunneling current decay between the STM tip and sample depends on the distance between the tip and sample, d_{gap}, and the decay rate of the tunnel junction between the tip and thiolate α, measured as the ATBH. Similarly, the tunneling current decays exponentially along the length of the alkyl chain backbone ($L_{backbone}$), noted as β. This decay is independent of the headgroup, thus β is the decay of the tunneling current per carbon atom in the alkyl chain.[22,23,31−33]

Previous work related the difference in apparent height in STM images between two different length alkanethiolate molecules to the differences in chain length, and thus differences in conductance.[22] Mixed alkaneselenolate monolayers of varying chain length and stoichiometry were made in order to test that the measured STM height difference (in constant current mode) is due to differences in the length and not properties of the headgroups. Measured STM height differences between molecules in these samples are summarized in Table 1.[34] From the data for both alkaneselenolate and alkanethiolate molecules, for a calculated physical height difference of ~2.2 Å between alkyl chain lengths of 10 and 12 carbons, a 1.1 Å STM apparent height difference is observed, as shown previously for thiolate headgroups.[22] This observation indicates that the headgroup has little effect on the current decay (β) through the alkyl backbone of the molecule, and that any observable difference between these molecules is due to the difference in the length of the molecule.

Mixed composition monolayers of decanethiolate and decaneselenolate (dodecyl chains were also studied) were prepared to probe the conductance differences between thiolates and selenolates. For most samples, high degrees of mixing were observed, resulting in structures composed of small domains of each type of molecule, as well as areas where no separation of component molecules was apparent. This indicates that the two headgroups have similar interfaces with the surface, as indicated by the similarity in the tilt-angles determined from X-ray diffraction, ellipsometry, and infrared spectroscopy.[3,35−38] Varied surface structures were observed, most of which do not resemble the ordered structures that both pure alkanethiolate and alkaneselenolate SAMs on Au{111} have previously been

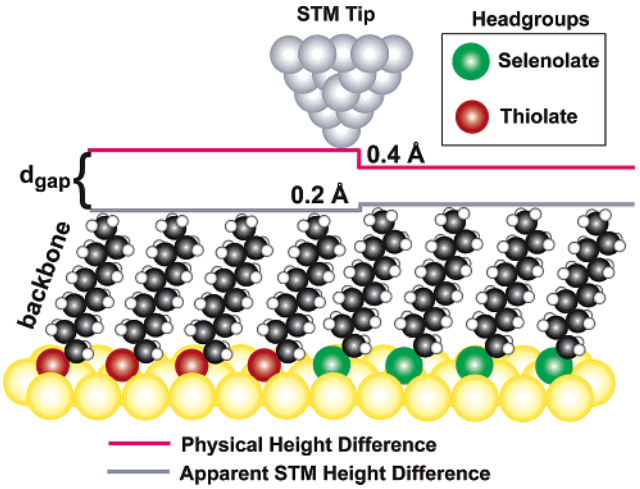

Figure 1. Schematic showing the different regimes through which an electron tunnels (gap, backbone, and headgroup). Using the covalent bond radii to carbon to calculate the difference in height between decanethiolate and decaneselenolate, the headgroups (selenium depicted in green and sulfur depicted in red) differ in diameter by 0.2 Å as indicated by the gray lines. The difference in contact conductance between the two termini results in an observed STM height difference of 0.4 Å is indicated by the red lines.

TABLE 1: Comparison of Experimentally Observed Apparent STM Height Differences between Different Length and Headgroup SAMs to the Physical Height Differences[a]

component 1	component 2	calcd physical height diff, Å	measd STM height diff, Å
$CH_3(CH_2)_9S-$	$CH_3(CH_2)_{11}S-$	2.20	1.1
$CH_3(CH_2)_9Se-$	$CH_3(CH_2)_{11}Se-$	2.20	1.1
$CH_3(CH_2)_9S-$	$CH_3(CH_2)_9Se-$	0.25	−0.4
$CH_3(CH_2)_{11}S-$	$CH_3(CH_2)_{11}Se-$	0.25	−0.4
$CH_3(CH_2)_9S-$	$CH_3(CH_2)_{11}Se-$	2.45	0.7
$CH_3(CH_2)_{11}S-$	$CH_3(CH_2)_9Se-$	−1.95	−1.5

[a] These differences are defined as the values for component 2 minus those for component 1, and are reported in columns 3 and 4. Listed are the components of the SAM, with the backbone length indicated in terms of number of carbon atoms. The calculated physical height differences between the two regions of each film are listed. The observed apparent topographic height differences are listed in the last column, indicating that there is a measured height difference of ca. −0.4 Å that arises and is attributed to a difference in headgroup conductance.

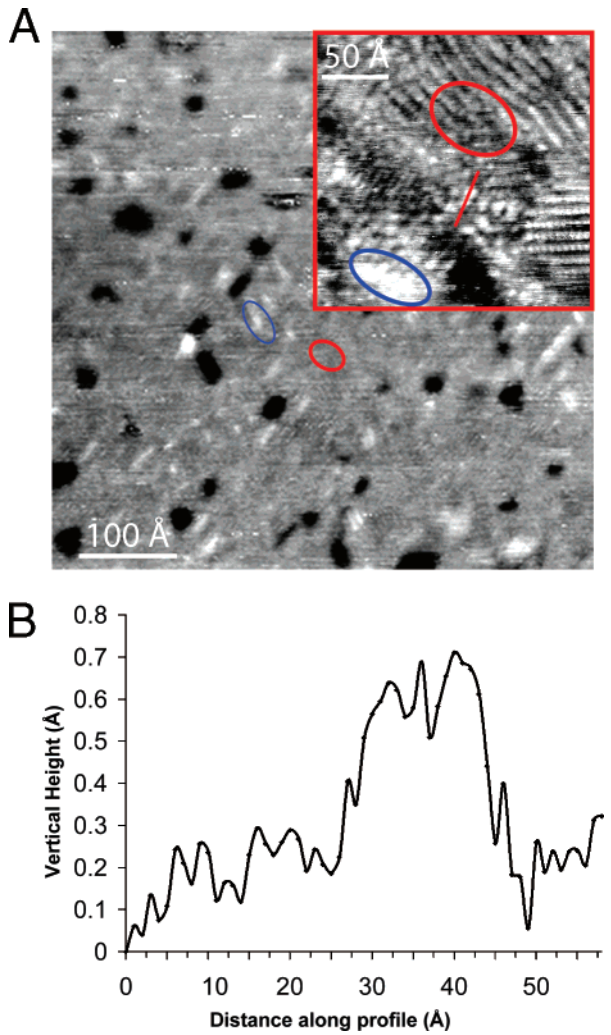

Figure 2. (A) STM image of a 550 × 550 Å^2 area of a mixed decaneselenolate and decanethiolate SAM on Au{111} prepared from a deposition solution with a 4:1 concentration ratio of selenol to thiol with a 200 × 200 Å^2 image inset, recorded at −1 V sample bias and 1.0 pA tunneling current. Decanethiolate (examples circled in blue) is topographically protruding relative to decaneselenolate (examples circled in red), as determined from the surface composition of this and other preparations. (B) Topographic height profile traced in red on the inset image indicating the apparent height difference found for the different molecules.

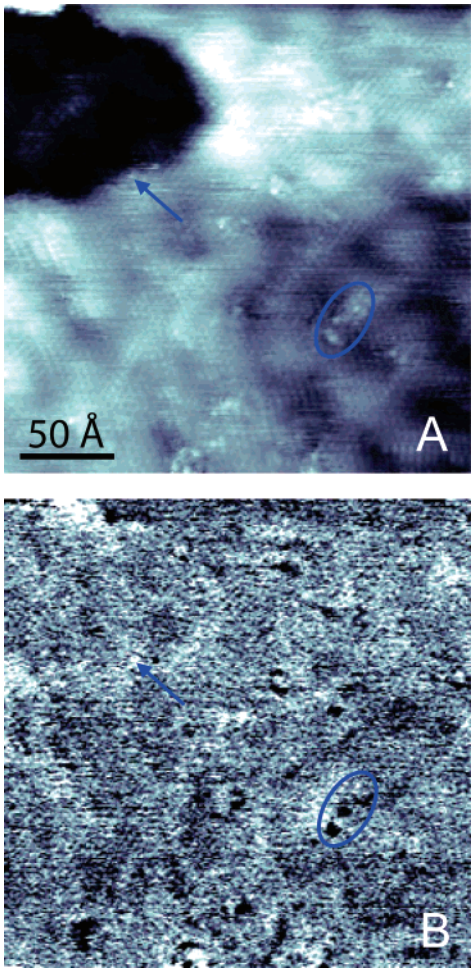

Figure 3. (A) STM and simultaneously acquired ATBH images of a 250 × 250 Å^2 area of a mixed decaneselenolate and decanethiolate SAM on Au{111} prepared from a deposition solution with a 4:1 concentration ratio of selenol to thiol acquired at −1 V sample bias and 1.0 pA tunneling current. The majority of the sample was decaneselenolate; it was identifiable from the characteristic Moiré pattern exhibited, which has previously been observed for selenolates but not for thiolates,[38] as well as determined by the stoichiometry of the overall surface composition. Decanethiolate (example circled in blue) was topographically protruding ∼0.4 Å relative to decaneselenolate in STM images. (B) ATBH image indicating that the thiolates had a lower apparent tunneling barrier height than selenolates. The blue arrow points to a substrate vacancy island defect, which has the highest observed ATBH.

shown to exhibit.[39−41] A 550 × 550 Å^2 STM image with a 200 × 200 Å^2 inset (Figure 2a) reveals areas of decanethiolates (circled in blue) and decaneselenolates (circled in red) that display differences in apparent STM topographic height. On the basis of population correlations with deposition solution concentration ratios, the protruding features are assigned as decanethiolate. The presence of Moiré patterns in STM images of samples prepared from deposition solutions with greater than 4:1 concentration ratios of decaneselenol to decanethiol (Figure 3) indicate that the majority of the surface molecules conform to structures characteristic of pure alkaneselenolate monolayers,[38] further confirming this assignment. STM images indicate that the two types of features observed differ by ∼0.4 Å in apparent height as indicated by a line profile across the sample (Figure 2b). However, using the covalent bond radii to carbon for both S and Se atoms to calculate the theoretical difference in physical height between identical alkyl chain length molecules, a decaneselenolate molecular film should be physically ∼0.2 Å thicker than a decanethiolate film.[10,42,43] Figure 1 illustrates this height difference, indicating the physical height difference due to the headgroup and the observed STM height difference.[44]

To corroborate these results, mixed length/mixed headgroup monolayers were made with varying compositions. These mixed monolayers show a smaller difference in measured STM height when the selenolate molecule is longer (i.e., dodecaneselenolate as compared to decanethiolate), and a larger difference in height when the selenolate molecule is shorter than the thiolate molecule. These results are summarized in Table 1. Previous measurements note a 1.1 Å difference in apparent STM height between decyl and dodecyl species,[22] therefore, any changes to this should be attributed to the molecule−metal linking group. The selenolate headgroup causes the molecule to be imaged ∼0.4 Å shorter than previously noted for the difference in apparent STM height between decanethiolate and dodecanethiolate species, yet a selenolate is calculated to be a longer molecule than a thiolate. Since the ∼0.4 Å measured topographic

height difference can be related solely to the headgroup, these measured height differences can be attributed to the headgroup's electronic interaction with the substrate, indicating that alkanethiolates have a higher contact conductance than alkaneselenolates.

Quantifying the difference in headgroup conductance requires information beyond the apparent STM topographic height differences. An experiment addressing the contact conductance difference between decanethiolate and decaneselenolate can be designed by using a detailed description of the current decay through each part of the molecule. The total conductance of a system comprised of two methylene backbones of the same length, one terminated with S and the other with Se, will vary by the different B factors for the two adsorbed molecules from eqs 1−3. Factor B describes the contact conductance between the molecule and the substrate, and thus contains information pertinent to the headgroup. However, differences in factor A (which describes the conductance interface between the tip and molecule, eqs 1 and 3) would be negligible if the methylene backbone is of the same composition and orientation. Consequently, the tip−sample interaction should not change from one molecule to the next. Likewise, changes in d_{gap} should be insignificant from one molecule to the next with little change to the local tip−sample interface, leaving α to be measured as the apparent tunneling barrier height. Therefore, to account for the difference in conductance between decanethiolate and decaneselenolate, both α and B need to be determined.

Measuring Apparent Tunneling Barrier Height. In constant current STM experiments, the ATBH is typically understood in terms of the tip sampling decay profile of a molecule's wave function. The current (I_t) conducted through the tunnel junction at an applied bias (V_t) can be approximated by:

$$I_t = G_t V_t \exp\left(\frac{8m_e}{\hbar^2}\sqrt{\bar{\phi}}\, z\right) \qquad (4)$$

where G_t is the contact conductance, $\bar{\phi}$ is the average ATBH, m_e is the mass of the electron, and z is the tip−sample separation.[23,27−30] By rearranging (4) and assuming constant V_t, the ATBH can be defined in terms of experimental observable quantities:

$$\bar{\phi} = \frac{\hbar^2}{8m_e}\left(\frac{\mathrm{d}\ln I}{\mathrm{d}z}\right)^2 = -0.952\ [\mathrm{eV\ \AA^2}]\left(\frac{\mathrm{d}\ln I}{\mathrm{d}z}\right)^2 \qquad (5)$$

the change in tunneling current with respect to the change in tip−sample separation.[27,45] Thus, the ATBH can be correlated to the modulation in the tunneling current with respect to the change in tip−sample separation.

Apparent tunneling barrier height has been used to assess conductance differences for many systems. It has been used in a comparative mode to compare nonanethiol and selected conjugated molecules.[46] In single component adsorbed monolayers, ATBH has been used to differentiate between binding sites, such as 3-fold hollow, bridge, and atop.[47] Applying ATBH measurements to the decanethiolate/decaneselenolate experiment, the decay of the entire tip−molecule system is probed, and by assuming the decay of the molecular backbone is independent of the headgroup (as shown above), it can be concluded that differences in α for the same length alkyl chain are unique to the headgroup and can be identified and fixed, allowing a better understanding of headgroup conductance.

The difference in ATBH can be used to differentiate species in mixed headgroup, same chain length samples (e.g., decanethiolate and decaneselenolate). Figure 3 shows representative images for such a sample, showing areas containing topographic protrusions (decanethiolate circled in red), regions bearing a characteristic Moiré pattern (decaneselenolate), as well as surface defect sites (indicated by a red arrow), all of which correspond to different ATBH values. By rank, the thiolates (topographically most protruding) have the lowest ATBH, followed by the selenolates, with the surface defects having the highest ATBH (indicated by a red arrow in Figure 3). Average ATBH values for identifiable regions of alkaneselenolates were 0.28 eV, compared to 0.269 eV measured for alkanethiolates. While these measurements reveal similar trends to those previously reported for the thermionic emission barrier for biphenyl-thiolate molecules at both positive and negative biases,[48] and calculations,[10] these numeric values should be viewed only on a comparative basis, since there is potential for variability in ATBH measurements acquired in air arising when the applied voltage (V_{app}) does not necessarily equal the tunneling gap voltage (V_{tg}).[27] With this caveat in mind, we reproducibly measure thiolates to have 0.01 eV smaller ATBH than selenolates. By using this information and β, the difference in contact conductance between thiolates and alkaneselenolates can be deduced.

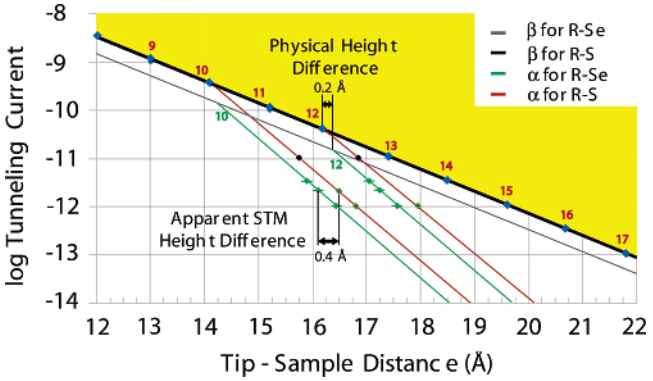

Figure 4. Semilogarithmic plots of the tunneling current vs tip−Au substrate separation for *n*-alkanethiolates and *n*-alkaneselenolates on Au{111} at a −1 V sample bias and tunneling currents as plotted (adapted from refs 22 and 32). The blue diamonds represent the hypothetical current−distance point for the tip just in contact with the ends of the methyl termini for the total number of carbons in the alkyl chain indicated. These diamonds fall on a line with a slope $-\beta/\ln(10) = -0.5$ Å^{-1} ($\beta = 1.2$ Å^{-1}), which represents the current decay versus the length of the alkyl chain. The yellow region above this line corresponds to the condition where the tip has penetrated the alkanethiolate film. The red lines intersecting the blue diamonds at alkyl chain lengths of 10 and 12 carbon atoms (and analogous green lines for alkaneselenolates) represent the tunneling current−distance relationship (for alkanethiolates and alkaneselenolates, respectively) when the tip is outside the SAM surface (beyond the ends of the alkanethiolate and alkaneselenolate chains) with the slopes indicative of the apparent tunneling barrier height. The measured STM topographic height differences between alkanethiolates and alkaneselenolates are plotted as green diamonds at the measured tunneling current set-point values of 1, 2, and 3 pA. Alkanethiolate data are plotted along the previously reported slope, while alkaneselenolate data are plotted at the measured distance shorter than the alkanethiolates (the alkaneselenolates appeared shorter in topographic image data and are plotted as green). The α-sloped (green) lines for alkaneselenolates are obtained by best fit lines through the observed data. The β-sloped (gray) line for alkaneselenolates is placed parallel to the one for alkanethiolates, intersecting the alkaneselenolate α-sloped line at a position ~0.20 Å longer than the one for alkanethiolates (this is to account for the difference in headgroup size between S and Se).

Quantifying Contact Conductance. The ratio of the contact conductances (B) between alkanethiolates and alkaneselenolates

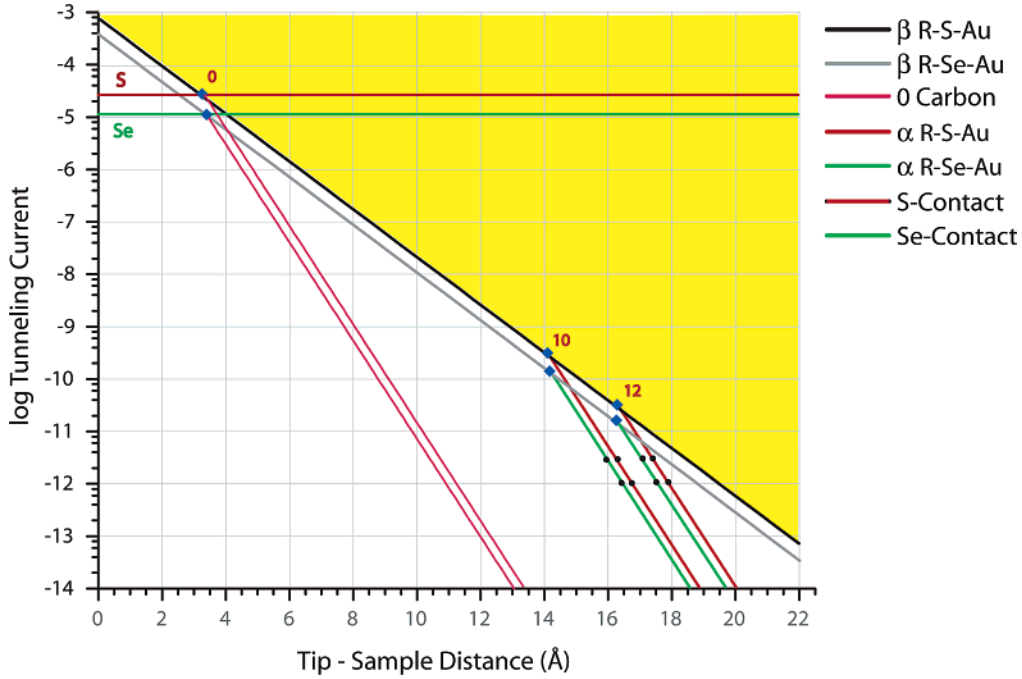

Figure 5. Semilogarithmic plot of the tunneling current vs tip−Au substrate separation for *n*-alkanethiolates and *n*-alkaneselenolates on Au{111} at a −1 V sample bias and tunneling currents as plotted, extrapolated to zero carbons in the alkyl chain. The resistance calculated by Ohm's law, using the tunneling current corresponding to zero carbons and 1 V, results in 33 kΩ for the thiolate headgroup and 83 kΩ for the selenolate headgroup.

can be determined by using eq 3 with knowledge of A, d_{gap}, $L_{backbone}$, α, and β. In a mixed headgroup SAM (e.g., for decanethiolate and decaneselenolate), where the alkyl chain length ($L_{backbone}$) is the same, both the orientation and chemistry of the methyl top contact are the same. Differences in contributions to conductance from the interactions between the tip and methyl termini at the tunneling gap should therefore be minimal, resulting in negligible change to A and d_{gap}. As a result, the only difference in the system is the headgroup (S vs Se), in size and chemistry. Since Se is a slightly larger atom (∼0.20 Å greater diameter when bound to carbon)[42,43] and more polarizable than S, Se should have different contact electronic properties, resulting in a different contact conductance, and only a slightly larger molecular length.[49]

To isolate the contributions to conductance of the headgroup from the aliphatic backbone and determine the difference in contact conductance between sulfur and selenium headgroups, the comparative height differences between alkanethiolates and alkaneselenolates at the measured tunneling currents were combined with previously reported data.[22] The results are shown as semilogarithmic plots of tunneling current vs tip−sample separation in Figure 4. The bold black line separating the yellow shaded region from the unshaded region represents the boundary between physical penetration of the film and tunneling through the gap between the tip and the tail ends of alkanethiolate molecules for a range of alkyl chain lengths. This line has the slope of $-\beta/\ln(10) = -0.5$ Å^{-1} ($\beta \approx 1.1$) and is the decay of the alkyl chain's electronic wave function. Outside the film (unshaded region), the current−distance relationship for alkanethiolates has a slope of $-\alpha/\ln(10) = -1.0$ Å^{-1} ($\alpha \approx 2.3$) and is represented by red lines. By using these red lines for alkaneselenolates as reference, the apparent topographic height differences (Table 1) between the alkanethiolates and alkaneselenolates at the measured tunneling currents were plotted as green diamonds and a best fit line was drawn. Since the α-sloped lines for alkaneselenolates are drawn through points that are a consistent distance from the points on the α-sloped lines for alkanethiolates, the resultant lines are parallel within experimental error. Measurements of α in this experiment resulted in $\alpha \approx 2.28$ for both thiolates and selenolates. When extrapolated to zero alkyl chain lengths, the tunneling current (Y-axis intercept) corresponding to the intersection of α- and β-sloped lines represents the contact conductance.

The contact conductance for alkaneselenolates can be inferred by extrapolating the α-sloped line for alkaneselenolates to zero alkyl chain lengths, as in Figure 5. Shown are α- and β-sloped lines for both thiolates and selenolates as in Figure 4 for measured values and slopes parallel for extrapolated zero carbon units. To account for the ∼0.20 Å difference in headgroup size, the position of a β-sloped line for alkaneselenolates (thin gray line) was lowered to the point where it intersected the best fit line (α for alkaneselenolates) at a distance 0.20 Å from the β-sloped line for alkanethiolates (thick black line).[50] If left unadjusted, the α-sloped lines for alkaneselenolates would intersect the original β-sloped line ∼0.40 Å to the left of the α-sloped lines for alkanethiolates, representing only the observed STM height differences, not both the observed STM and calculated physical height difference between the molecules. The conductance differences that would result in the measured topographic height difference (∼0.40 Å) are of the magnitude that is represented by lowering the β-sloped line to account for the decrease in B.[22] Therefore, having adjusted for the physical height difference between the headgroups, the majority of the difference in apparent STM tunneling height is due to the differences in the contact conductance.

By using Ohm's law at a constant voltage (all the data used for this analysis were acquired at a sample bias of −1 V) and the current predicted by the extrapolation, the effective contact resistance for Au−Se−R is ∼83 kΩ and that for Au−S−R is ∼33 kΩ. We note that these are approximate multiples of the Landauer resistance ($2e^2/h \approx 13$ kΩ).[51] Thus, alkanethiolates are 2.5 times more conductive than alkaneselenolates. Beebe et al. used conductive probe atomic force microscopy and extrapolation in a similar fashion, and have reported ∼18.5 kΩ

for thiolate−Au terminations,[11] which is within experimental error of our results.

The difference in conductance between alkanethiolates and alkaneselenolates may be explained by considering the differences in the chemistry between S vs Se on the Au substrate. X-ray photoelectron spectroscopy and nuclear magnetic resonance data of alkaneselenolate and alkanethiolate moieties adsorbed on Au nanoparticles indicate that the Au−Se bond is stronger and more covalent than the Au−S bond.[52,53] Se is also more polarizable than S, therefore a higher barrier to conductance via a surface dipole may be set up for Se than for S. Further, the HOMO-LUMO gap of an alkyl chain bound to a surface may be better mediated by S compared to Se.[10,54,55] The HOMO-LUMO gap for alkanethiolate SAMs on Au is typically taken to be ∼8 eV;[55] there is no equivalent value for alkaneselenolate SAMs on Au, but it is expected to be somewhat smaller based on periodic trends. Arenechalcogenide conductance has been treated theoretically by Di Ventra and Lang,[56] and band alignment was found to play a critical role. For *p*-dichalcogenobenzenes attached to two Au electrodes modeled by Jellium (with the electron density of metallic gold, $r_S = 3$), the thiolate headgroup/Au Fermi level lies closer to the molecules' LUMO than the HOMO, and the Se headgroup/Au Fermi level lies very close to the HOMO. This band alignment was found to be the critical parameter in predicting higher conductance for conjugated selenolates. Band alignment arguments were also given as the underlying reason that benzenethiolate on Au was predicted to be more conductive than benzeneselenolate by Seminario et al.[10] For α,α′-xylyldichalcogenides between Au electrodes, Yaliraki et al. attributed the predicted higher conductance of dithiolate vs diselenolate to a combination of band alignment, gap, and intramolecular orbital mixing.[9] The band alignment of the alkylthiolates vs the alkylselenolates on Au is not known, but is critical to understanding the conductance order and ratio found here. Likewise, as noted in ref 9, the mixing of the headgroup with the backbone orbitals plays a role that is not straightforwardly predictable.

Conclusions

By comparing identical alkyl chain length alkanethiolates and alkaneselenolates, we observe that even though alkaneselenolate films are calculated to be physically ∼0.20 Å thicker, in STM images they appeared ∼0.4 Å less protruding than alkanethiolates. Using ATBH imaging, we have been able to separate conductances of molecular species with the same alkyl chain length from topographic information. We have shown that both the topographic height and ATBH differences are predominantly due to the difference in contact conductance between the two chalcogenate species. This difference in contact conductance amounts to a factor of 2.5, with alkanethiolates more conductive than equivalent alkaneselenolates. Consequently, for these molecules attached to Au{111} surfaces, R−S−Au makes a more conductive contact than R−Se−Au.

Acknowledgment. The authors would like to thank Drs. Lloyd Bumm, Massimiliano Di Ventra, Daniel Fuchs, Christian Joachim, Kevin Kelly, Norton Lang, and Brent Mantooth for helpful discussions. Support is gratefully acknowledged from DARPA, NIST, NSF, and ONR.

Supporting Information Available: STM images, linescans, histograms of height distributions for differences in topographic STM height. This material is available free of charge via the Internet at http://pubs.acs.org.

References and Notes

(1) Allara, D. L.; Dunbar, T. D.; Weiss, P. S.; Bumm, L. A.; Cygan, M. T.; Tour, J. M.; Reinerth, W. A.; Yao, Y.; Kozaki, M.; Jones, L., II *Ann. N. Y. Acad. Sci.* **1998**, *852*, 349.

(2) Weiss, P. S.; Bumm, L. A.; Dunbar, T. D.; Burgin, T. P.; Tour, J. M.; Allara, D. L. *Ann. N. Y. Acad. Sci.* **1998**, *852*, 145.

(3) Samant, M. G.; Brown, C. A.; Gordon, J. G., II *Langmuir* **1992**, *8*, 1615.

(4) Bain, C. D.; Troughton, E. B.; Tao, Y. T.; Evall, J.; Whitesides, G. M.; Nuzzo, R. G. *J. Am. Chem. Soc.* **1989**, *111*, 321.

(5) Henderson, J. I.; Feng, S.; Ferrence, G. M.; Bein, T.; Kubiak, C. P. *Inorg. Chim. Acta* **1996**, *242*, 115.

(6) Sachs, S. B.; Dudek, S. P.; Hsung, R. P.; Sita, L. R.; Smalley, J. F.; Newton, M. D.; Feldberg, S. W.; Chidsey, C. E. D. *J. Am. Chem. Soc.* **1997**, *119*, 10563.

(7) Frey, S.; Shaporenko, A.; Zharnikov, M.; Harder, P.; Allara, D. L. *J. Phys. Chem. B* **2003**, *107*, 7716.

(8) Stewart, M. P.; Maya, F.; Kosynkin, D. V.; Dirk, S. M.; Stapleton, J. J.; McGuiness, C. L.; Allara, D. L.; Tour, J. M. *J. Am. Chem. Soc.* **2004**, *126*, 370.

(9) Yaliraki, S. N.; Kemp, M.; Ratner, M. A. *J. Am. Chem. Soc.* **1999**, *121*, 3428.

(10) Seminario, J. M.; Zacarias, A. G.; Tour, J. M. *J. Am. Chem. Soc.* **1999**, *121*, 411.

(11) Beebe, J. M.; Engelkes, V. B.; Miller, L. L.; Frisbie, C. D. *J. Am. Chem. Soc.* **2002**, *124*, 11268.

(12) Cui, X. D.; Primak, A.; Zarate, X.; Tomfohr, J.; Sankey, O. F.; Moore, A. L.; Moore, T. A.; Gust, D.; Harris, G.; Lindsay, S. M. *Science* **2001**, *294*, 571.

(13) Cui, X. D.; Primak, A.; Zarate, X.; Tomfohr, J.; Sankey, O. F.; Moore, A. L.; Moore, T. A.; Gust, D.; Nagahara, L. A.; Lindsay, S. M. *J. Phys. Chem. B* **2002**, *106*, 8609.

(14) Chen, J.; Wang, W.; Reed, M. A.; Rawlett, A. M.; Price, D. W.; Tour, J. M. *Appl. Phys. Lett.* **2000**, *77*, 1224.

(15) Cai, L. T.; Skulason, H.; Kushmerick, J. G.; Pollack, S. K.; Naciri, J.; Shashidhar, R.; Allara, D. L.; Mallouk, T. E.; Mayer, T. S. *J. Phys. Chem. B* **2004**, *108*, 2827.

(16) Chen, J.; Reed, M. A.; Rawlett, A. M.; Tour, J. M. *Science* **1999**, *286*, 1550.

(17) Reed, M. A.; Chen, J.; Rawlett, A. M.; Price, D. W.; Tour, J. M. *Appl. Phys. Lett.* **2001**, *78*, 3735.

(18) Kushmerick, J. G.; Holt, D. B.; Yang, J. C.; Naciri, J.; Moore, M. H.; Shashidhar, R. *Phys. Rev. Lett.* **2002**, *89*, 086802.

(19) Xu, B.; Tao, N. J. *Science* **2003**, *301*, 1221.

(20) Selzer, Y.; Cabassi, M. A.; Mayer, T. S.; Allara, D. L. *J. Am. Chem. Soc.* **2004**, *126*, 4052.

(21) Selzer, Y.; Cabassi, M. A.; Mayer, T. S.; Allara, D. L. *Nanotechnology* **2004**, *15*, S483.

(22) Bumm, L. A.; Arnold, J. J.; Dunbar, T. D.; Allara, D. L.; Weiss, P. S. *J. Phys. Chem. B* **1999**, *103*, 8122.

(23) Magoga, M.; Joachim, C. *Phys. Rev. B* **1997**, *56*, 4722.

(24) Gladysz, J. A.; Hornby, J. L.; Garbe, J. E. *J. Org. Chem.* **1978**, *43*, 1204.

(25) Reinerth, W. A.; Tour, J. M. *J. Org. Chem.* **1998**, *63*, 2397.

(26) Bumm, L. A.; Arnold, J. J.; Charles, L. F.; Dunbar, T. D.; Allara, D. L.; Weiss, P. S. *J. Am. Chem. Soc.* **1999**, *121*, 8017.

(27) Olesen, L.; Brandbyge, M.; Sorensen, M. R.; Jacobsen, K. W.; Laegsgaard, E.; Stensgaard, I.; Besenbacher, F. *Phys. Rev. Lett.* **1996**, *76*, 1485.

(28) Probst, O. M. *Am. J. Phys.* **2002**, *70*, 1110.

(29) Lang, N. D. *Phys. Rev. B* **1988**, *37*, 10395.

(30) Simmons, J. G. *J. Appl. Phys.* **1963**, *34*, 1793.

(31) Tomfohr, J.; Sankey, O. F. *J. Chem. Phys.* **2004**, *120*, 1542.

(32) Salmeron, M.; Neubauer, G.; Folch, A.; Tomitori, M.; Ogletree, D. F.; Sautet, P. *Langmuir* **1993**, *9*, 3600.

(33) Hong, S.; Reifenberger, R.; Tian, W.; Datta, S.; Henderson, J.; Kubiak, C. P. *Superlattices Microstruct.* **2000**, *28*, 289.

(34) Supplemental figures illustrating these topographic height differences are available on the web in the Supporting Information.

(35) Samant, M. G.; Brown, C. A.; Gordon, J. G., II *Langmuir* **1991**, *7*, 437.

(36) Porter, M. D.; Bright, T. B.; Allara, D. L.; Chidsey, C. E. D. *J. Am. Chem. Soc.* **1987**, *109*, 3559−3568.

(37) Dubois, L. H.; Nuzzo, R. G. *Annu. Rev. Phys. Chem.* **1992**, *43*, 437−463.

(38) Monnell, J. D.; Stapleton, J. J.; Jackiw, J. J.; Dunbar, T. D.; Reinerth, W. A.; Dirk, S. M.; Tour, J. M.; Allara, D. L.; Weiss, P. S. *J. Phys. Chem. B* **2004**, *108*, 9834.

(39) Monnell, J. D.; Stapleton, J. J.; Jackiw, J. J.; Dunbar, T. D.; Reinerth, W. A.; Dirk, S. M.; Tour, J. M.; Allara, D. L.; Weiss, P. S. *J. Phys. Chem. B* **2004**, *108*, 9834.

(40) Poirier, G. E. *Langmuir* **1999**, *15*, 1167.

(41) Poirier, G. E.; Tarlov, M. J. *Langmuir* **1994**, *10*, 2853.
(42) *CRC Handbook of Chemistry and Physics*, 84th ed.; Lide, D. R., Ed.; CRC Press LLC: Boca Raton, FL, 2003; p 2616.
(43) Oilunkaniemi, R.; Laitinen, R. S.; Ahlgren, M. *Z. Naturforsch. B: Chem. Sci.* **2000**, *55*, 361.
(44) A discussion of the feedback mechanism and imaging mixed height molecules with STM can be found in ref 22.
(45) Chen, C. J.; Hamers, R. J. *J. Vac. Sci. Technol. B* **1991**, *9*, 503.
(46) Ishida, T.; Mizutani, W.; Choi, N.; Akiba, U.; Fujihira, M.; Tokumoto, H. *J. Phys. Chem. B* **2000**, *104*, 11680.
(47) Sasaki, M.; Yamada, Y.; Ogiwara, Y.; Yagyu, S.; Yamamoto, S. *Phys. Rev. B* **2000**, *61*, 15653.
(48) Tour, J. M.; Reinerth, W. A.; Jones, L.; Burgin, T. P.; Zhou, C. W.; Muller, C. J.; Deshpande, M. R.; Reed, M. A. *Ann. N. Y. Acad. Sci.* **1998**, *852*, 197.
(49) In previous reports, the diameter of the headgroup has been included in the length of the molecule, hence when comparing alkanethiolates to alkaneselenolates, we add 0.2 Å to the length of the molecule for alkaneselenolates.
(50) Confirmation that β observed for alkaneselenolates is comparable to that previously observed for alkanethiolates was shown above.
(51) Holcomb, D. F. *Am. J. Phys.* **1999**, *67*, 278.
(52) Lee, C. K.; Ulman, A.; Ruiz, J. D.; Parikh, A.; White, H.; Rafailovich, M. *Langmuir* **2003**, *19*, 9450.
(53) Zelakiewicz, B. S.; Yonezawa, T.; Tong, Y. *J. Am. Chem. Soc.* **2004**, *126*, 8112.
(54) Joachim, C.; Magoga, M. *Chem. Phys.* **2002**, *281*, 347.
(55) Wang, W.; Lee, T.; Reed, M. A. *Phys. Rev. B* **2003**, *68*, 035416.
(56) Di Ventra, M.; Lang, N. D. *Phys. Rev. B* **2001**, *65*, 045402.